



Development of navigation network revealed by resting-state and task-state functional connectivity

Xin Hao^{a,b}, Taicheng Huang^c, Yiyong Song^{c,*}, Xiangzhen Kong^d, Jia Liu^{e,*}

^a Key Laboratory of Adolescent Cyberpsychology and Behavior (Central China Normal University), Ministry of Education, Wuhan, China

^b School of Psychology, Central China Normal University, Wuhan, China

^c Beijing Key Laboratory of Applied Experimental Psychology, Faculty of Psychology, Beijing Normal University, Beijing, China

^d Department of Psychology and Behavioral Sciences, Zhejiang University, Hangzhou, China

^e Department of Psychology & Tsinghua Laboratory of Brain and Intelligence, Tsinghua University, Beijing, China

ARTICLE INFO

Keywords:

Development
Navigation network
Functional connectivity
Resting-state
Task-state

ABSTRACT

Humans possess the essential capacity to navigate in environment, supported by multiple brain regions constituting the navigation network. Recent studies on development of the navigation network mainly examined activation changes in the medial temporal regions. It is unclear how the large-scale organization of the whole navigation network develops and whether the network organizations under resting-state and task-state develop differently. We addressed these questions by examining functional connectivity (FC) of the navigation network in 122 children (10-13 years) and 260 adults. First, we identified a modular structure in the navigation network during resting-state that included a ventral and a dorsal module. Then, we found that the intrinsic modular structure was strengthened from children to adults, that is, adults showed stronger FC within the ventral module and weaker FC between ventral and dorsal modules than children. Further, the intrinsic modular structure was loosened when performing scene-viewing task, that is, both adults and children showed decreased within-ventral FC and increased between-module FC during task- than resting-state. Finally, the task-modulated FC changes were greater in adults than in children. In sum, our study reveals age-related changes in the navigation network organization as increasing modularity under resting-state and increasing flexibility under task-state.

1. Introduction

Humans possess the essential capacity to navigate freely in the surrounding environment, which results from development of its underlying neural basis. fMRI studies in adults have identified multiple brain regions involved in spatial navigation, including the hippocampus (HIP) and entorhinal cortex in the medial temporal lobe (MTL), the scene-selective regions such as the parahippocampal place area (PPA), retrosplenial complex (RSC) and occipital place area (OPA), and some frontal-parietal regions such as the prefrontal cortex and the inferior parietal lobe (Bonner and Epstein, 2017; Burgess, 2006; Epstein et al., 2017; Epstein and Vass, 2014; Julian et al., 2016; Kamps et al., 2016; Spiers and Barry, 2015). Extensive functional connections (FCs) among the MTL and other navigational regions under both resting- and task-state have been observed, which constitute the navigation network. For example, intrinsic FCs among the HIP and scene-selective regions including the PPA and RSC, and task-evoked FCs between the HIP and prefrontal cortex have been reported (Boccia et al., 2016; Brown et al., 2016; Hao et al., 2017; Kong et al., 2016a). Furthermore, recent stud-

ies demonstrate differential connectivity patterns as a function within the posterior-anterior PPA, that is, the posterior PPA is more strongly connected to the OPA, while the anterior PPA is connected to the RSC and the caudal inferior parietal lobule (Baldassano et al., 2013; 2016). Despite plenty of research on the navigational network in adults, the development of the navigation network from children to adults has been relatively less investigated.

Previous developmental studies on the navigation network mainly examined age-related changes in fMRI activation during scene-related tasks in the scene-selective regions and MTL regions, but contradictory results have been reported. In particular, age-related increases of scene selectivity in the PPA and OPA (Golarai et al., 2007; Meissner et al., 2019) and increases of the PPA activation for successful scene memory (Chai et al., 2010) indicate a prolonged maturation process, whereas no age-related changes in scene selectivity in the RSC (Meissner et al., 2019) and PPA (Scherf et al., 2007) or in the HIP activation related to scene encoding (Ofen et al., 2007) indicate adult-level activation in children, and even age-related decreased activation in the left HIP and en-

* Corresponding author at: Faculty of Psychology, Beijing Normal University, 19 Xijiekouwai St, Haidian District, Beijing 100875, China.

E-mail addresses: songyiyong@bnu.edu.cn (Y. Song), liujiathu@tsinghua.edu.cn (J. Liu).

torhinal cortex during scene encoding has been reported (Menon et al., 2005).

It is not yet clear what principles underlie these inconsistent developmental differences in task-related activation, but evidence suggests that diverse network connectivity profiles may drive the related activation patterns and behaviors (Mahon and Caramazza, 2011; Saygin et al., 2016; Song et al., 2015). However, only a few studies have investigated the development of the navigation network connectivity, and they focus on the navigational task-related FCs between the MTL and frontal-parietal regions but with ambiguous findings. To be specific, increased FC with age has been found between the PPA and prefrontal regions during correct identification of studied scenes (Ofen et al., 2012), as well as between the entorhinal sub-region and dorsolateral PFC during encoding scenes (Menon et al., 2005). Inversely, decreased FC with age between the RSC and parietal regions is found during the remember-scene-ignore-face task (Jiang et al., 2014). These inconsistent findings suggest possible dissociable development trajectories for different FCs in the navigation network. Thus, it is important to investigate the development of large-scale functional organization of the navigation network from the whole network view. Notably, from a whole view, a stable modular structure has been identified for the navigation network in adults, with the medial temporal regions and dorsal regions constituting two distinct modules (Hao et al., 2016; Kong et al., 2016b). Thus, different modules of the navigation network may undergo distinct development trajectories, leading to development reorganization of the modular structure. Here, we investigated how such a functional modular organization of the navigation network develops from children to adults.

In particular, we examined the development of the functional organization of the whole navigation network under both resting-state and task-state in 122 children (10-13 years) and 260 adults. Many behavioral studies have shown adult-level performances in various navigation tasks such as allocentric navigation strategy, cue integration, and cognitive map representation around 11-12 years of age (Bullens et al., 2010; Burles et al., 2020; Julian et al., 2019; Nardini et al., 2008; Nazareth et al., 2018). On the other hand, findings regarding the neural development of navigation are mixed, and a number of studies have reported age-related changes in regional activation and functional interactions between regions after 12 years old until adulthood (Chai et al., 2010; Jiang et al., 2014; Meissner et al., 2019; Menon 2005; Ofen et al., 2012), suggesting a prolonged developmental trajectory for the neural basis of navigation. Therefore, we compared children aged 10-13 with adults to explore the possible prolonged development of the functional organization of the navigation network. While resting-state FC based on spontaneous synchronization reveals intrinsic organization of functional systems (Biswal et al., 1995; Fox and Raichle, 2007), task-evoked FC driven by a specific task exhibits transient changes of functional organization (Cassidy et al., 2016; Cole et al., 2014). First, we defined the navigation network across the whole brain and identified its modular structure. Second, we examined the development changes of the intrinsic network organization by examining the age-related changes in resting-state FCs within each module and between modules. Third, we explored the task modulation effect of network organization by calculating the FC changes from resting-state to task-state during a scene viewing task for each age group. Finally, we characterized the developmental trend of the task-evoked network organization by examining the age differences of the task modulation effect.

2. Materials and Methods

2.1. Participants

Participants included 122 children (age range: 10-13; mean age = 11.32, $SD = 0.75$ year, 59 males), 260 adults (age range: 18-25; mean age = 21.67, $SD = 1.03$ years, 127 males). Children were recruited from primary schools in Beijing through advertisements in school news-

papers and parents committee, and adults were recruited from Beijing Normal University. All participants were healthy with no history of neurological or psychiatric disorders. This study is part of an ongoing project (Gene Environment Brain & Behavior) (Kong et al., 2016a; Wang et al., 2016; Zhen et al., 2015). Before the experiment, all adult participants gave written informed consent; children gave their verbal informed consent and their primary caregiver provided written informed consent for them. All experimental procedures complied with the standards of the Institutional Review Board of Beijing Normal University. Twelve children participants were excluded with the exclusion criteria of mean framewise displacements (FD) > 0.3 mm or mean BOLD data variance (DVARs) > 3% under either resting-state or task-state (Ciric et al., 2017; Parkes et al., 2018; Power et al., 2012).

2.2. Navigation network construction

To identify a comprehensive and unbiased brain network involving in navigation, we chose the Neurosynth (<http://neurosynth.org>), a meta-analysis approach to define the navigation network (for details please see Hao et al., 2017). This approach utilizes term-based and machine-learning techniques to perform probabilistic mapping between neural activation and cognitive function (Yarkoni et al., 2011). Despite the automaticity and potentially high noise resulting from the association between term frequency and coordinate tables, this approach has been shown to be quite robust and reliable (Lebedev et al., 2014; Helfinstein et al., 2014). We searched for the keyword “navigation” in the database and adopted the resulting uniformity test map with a whole-brain false discovery rate (FDR) threshold of 0.01 to cover regions that are highly relevant to navigation tasks. To define a stable navigation network, only the clusters larger than 100 voxels in the resulting “navigation” probabilistic map were identified for further analysis (Kong et al., 2016a). As a result, 23 regions were included in the navigation network (Table 1). Some regions previously reported to be involved in spatial processing (e.g., medial prefrontal cortex, insula) were not included here due to their low activation probabilities across studies. We have confirmed the validity of the Neurosynth-defined navigation network by examining the relationship between the regions identified from Neurosynth and the well-established scene-selective regions in another study (Hao et al., 2017; Zhen et al., 2017). Finally, we described these regions using their corresponding labels in the automated anatomical labeling (AAL) atlas (Tzourio-Mazoyer et al., 2002).

2.3. fMRI Scanning and Image acquisition

Each participant completed a resting-state run and three task-state runs. To eliminate the possibility that participants might think about any stimulus in the resting-state runs, the resting-state run was conducted before the task-state runs. For the 8-min resting-state fMRI scanning, the participants were instructed to remain awake, keep still, close their eyes, and not think about any specific things. Each participant was asked whether he/she had fallen asleep during the scan, and those who reported having been asleep were asked to complete the resting-state fMRI for a second time. For the task-state fMRI scanning, the participants were instructed to passively view the movie clips containing scenes, faces, objects, or scrambled objects (for more details, see Hao et al., 2016; Zhen et al., 2015; Wang et al., 2017). The task-state scanning contained 3 blocked-design runs, and each of them lasted 198 s. Every run contained 2 block sets (each block set consisted of four blocks with each stimulus category) and 3 blocks of fixation at the beginning, middle, and end of the run. Each block lasted 18s for fixation or any stimulus category, and each stimulus category block contained six 3s movie clips.

MRI scanning was performed on a Siemens 3T scanner (MAGENTOM Trio, a Tim system) with a 12-channel phased-array head coil at Beijing Normal University Imaging Center for Brain Research, Beijing, China. The high-resolution T1-weighted structure images were acquired using a magnetization-prepared rapid gradient-echo (MPRAGE) sequence

Table 1
The Neurosynth-defined regions in navigation network.

Anatomical label	Hemisphere	Abbrevia-tion	Average Z score	Peak MNI coordinate			Voxel number	Module
				X	Y	Z		
Hippocampus	L	HIP.L	4.92	-24	-16	-20	181	ventral
	R	HIP.R	5.01	24	-14	-18	204	ventral
Parahippocampus gyrus	L	PHG.L	5.12	-26	-42	-8	156	ventral
	R	PHG.R	5.43	24	-40	-8	333	ventral
Retrosplenial cortex	L	RSC.L	4.63	-12	-56	6	125	ventral
	R	RSC.R	5.46	14	-54	12	170	ventral
Lingual gyrus	L	LING.L	5.04	-26	-48	-8	218	ventral
	R	LING.R	5.17	22	-42	-8	206	ventral
Fusiform gyrus	L	FFG.L	5.34	-28	-46	-10	354	ventral
	R	FFG.R	6.73	30	-40	-16	416	ventral
Middle occipital gyrus	L	MOG.L	4.44	-32	-74	30	209	dorsal
	R	MOG.R	4.81	36	-74	32	313	dorsal
Superior parietal gyrus	L	SPG.L	5.02	-20	-66	56	192	dorsal
	R	SPG.R	5.07	14	-66	56	131	dorsal
Inferior parietal lobe	L	IPL.L	4.76	-34	-62	40	184	dorsal
	R	IPL.R	4.74	36	-46	40	181	dorsal
Precuneus	L	PCUN.L	4.54	-8	-62	56	199	dorsal
	R	PCUN.R	5.03	12	-62	56	292	dorsal
Angular gyrus	R	ANG.R	5.05	32	-56	46	111	dorsal
Precentral gyrus	L	PreCG.L	5.31	-28	-4	56	168	dorsal
Superior frontal gyrus	R	SFG.R	5.72	26	2	56	152	dorsal
Middle frontal gyrus	L	MFG.L	5.76	-28	-2	56	120	dorsal
Supplementary motor area	L	SMA.L	5.52	-2	10	52	177	dorsal

(TR/TE/TI = 2.53s /3.39s/1.1s, FA = 7°, matrix = 256 × 256, voxel size = 1 mm × 1 mm × 1.33 mm, number of slices = 128) for each participant. The resting-state fMRI was scanned using a T2*-weighted gradient-echo echo-planar-imaging (GRE-EPI) sequence (TR/TE = 2s /30ms, FA = 90°, voxel size = 3.125 mm × 3.125 mm × 3.6 mm, number of slices = 33). The task-state fMRI was acquired using the T2*-weighted GRE-EPI sequence with different sequence parameters from resting-state fMRI (TR/TE = 2s /30ms, FA = 90°, voxel size = 3.125 mm × 3.125 mm × 4.8 mm, number of slices = 30).

2.4. fMRI Data Analysis

2.4.1. Resting-state fMRI data preprocessing and FC analysis

For each participant, image preprocessing of resting-state fMRI data was performed with FSL (FMRIB software Library, <http://www.fmrib.ox.ac.uk/fsl/>), including the removal of the first four volumes, head motion correction (by aligning each volume to the middle volume of the 4-D image with MCFLIRT), spatial smoothing (with a Gaussian kernel of 6 mm full-width at half-maximum, FWHM), intensity normalization, removal of linear trend, band-pass temporal filtering (0.01-0.1 Hz), and elimination of physiological noise (such as fluctuations caused by head motion, cardiac and respiratory cycles). As described in previous studies (Biswal et al., 2010; Fox et al., 2005), nuisance signals from the cerebrospinal fluid, white matter, global brain average, six head motion correction parameters, and first derivatives of these signals were regressed out in this study. Following preprocessing steps, the ROI-to-ROI FC analysis using the CONN functional connectivity toolbox (version v16.b) (Whitfield-Gabrieli and Nieto-Castanon, 2012) was carried out. The strength of the intrinsic FC between each pair of identified regions was estimated using the Pearson's correlation coefficients (r) of the 4-D residual resting-state fMRI time series.

2.4.2. Definition of ventral module and dorsal module

Then, we explored the modular structure of the navigation network by using the modularity analysis. Specifically, we firstly calculated the intrinsic group-averaged correlation matrix across adults. Then, using the community Louvain algorithm in the brain connectivity toolbox (BCT) (version 2017-01-15) (Rubinov and Sporns, 2010) with the default resolution parameter $\gamma = 1$ and 1,000 times run, we ob-

tained auto-generated optimal community structure with a module partition number of 2. Through further spatial location examination, we found that most regions in one of the modules were located in the ventral visual stream, which projects to the inferior temporal cortex (Ungerleider, 1982), including the HIP, parahippocampus gyrus (PHG), lingual gyrus (LING), and fusiform gyrus (FFG) and so on. Therefore, we labeled this module as the ventral module (Table 1). The other module contained a set of parietal-frontal regions, such as the middle frontal gyrus, inferior parietal lobe, superior parietal gyrus, supplementary motor area and middle occipital gyrus, which were mainly located in the dorsal visual stream (Kravitz et al., 2011), thus we labeled it as the dorsal module (Table 1). As a result, the ventral module consisted of 10 regions, and the dorsal module contained 13 regions (Table 1).

To further characterize the intrinsic modular structure of navigation network in adults, we calculated the resting-state FCs within each module and that between the two modules for each adult. Specifically, the within-ventral FCs were defined as the FCs between each pair of regions within the ventral module (upper left of the matrix, Fig. 1A, left). Similarly, the within-dorsal FCs were defined as the FCs between each pair of regions within the dorsal module (bottom right of the matrix, Fig. 1A, left). The between-module FCs were calculated as the FCs between each region in ventral module and each region in dorsal module (upper right and bottom left of the matrix, Fig. 1A, left). Then, for each participant, all the FC values belonging to each category were averaged, resulting in three averaged FC measures: within-ventral FC, within-dorsal FC, and between-module FC (Fig. 1A, right). Additionally, the FC matrices were averaged across all participants in the adults group to yield the group-average FC matrix for adults (Fig. 1A, left).

2.4.3. Age-related changes of intrinsic modular structure of the navigation network

To investigate age-related changes of intrinsic modular structure, we calculated the within- and between-module FCs for the children group (Fig. 1B) using the same methods as for adults. Then, we conducted non-parametric permutation tests to examine the group differences in FCs between adults and children (Nichols and Holmes, 2002). For each permutation test, we randomly reallocated all the values into adults and children and recalculated the mean differences between the two groups. This permutation procedure was repeated 10,000 times to form a null distribution and the 95th percentile points of null distribution was used

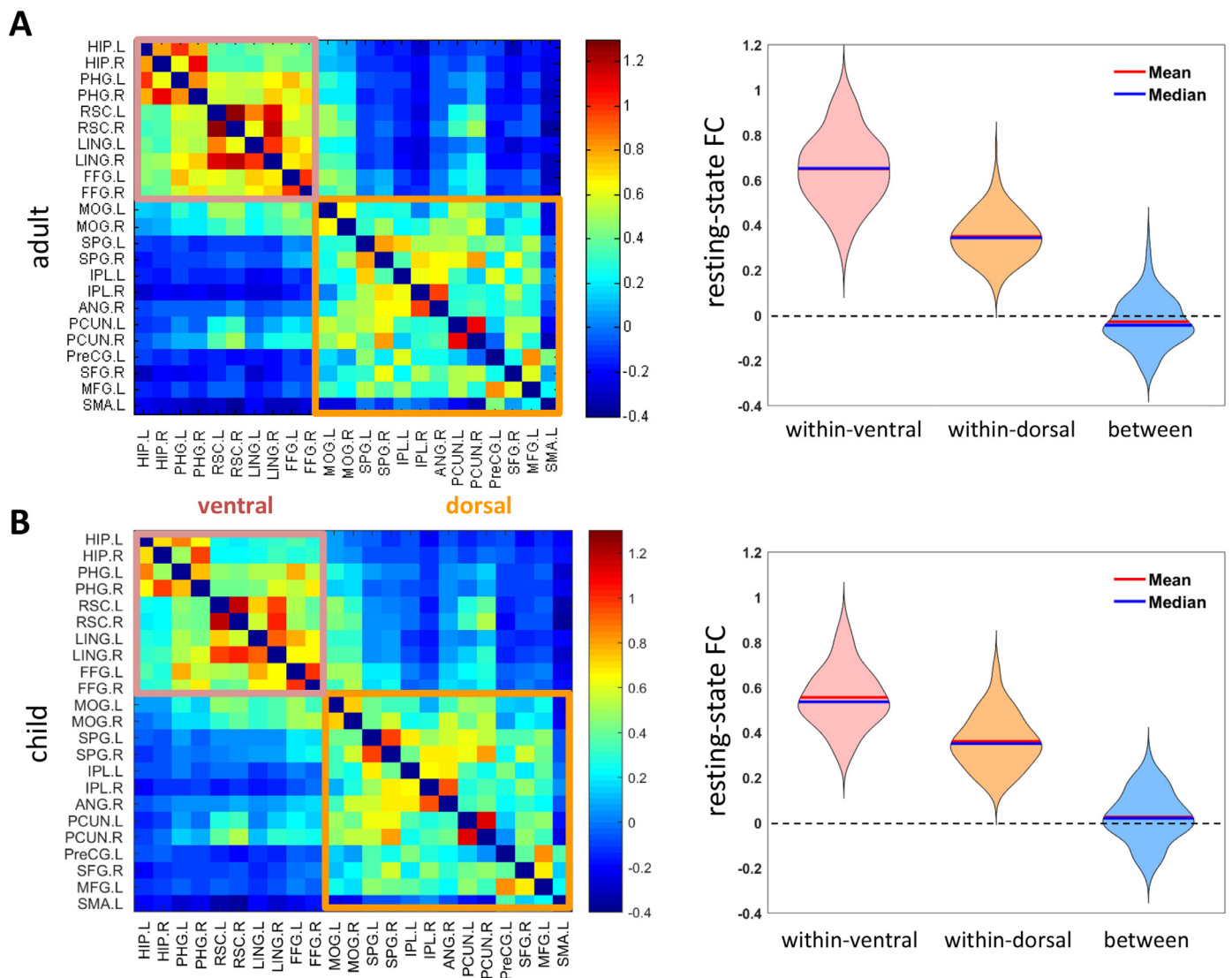


Fig. 1. Intrinsic FC profiles of navigation network in adults (A) and children (B). Left: The group-averaged resting-state FC matrix of the navigation network. We identified a ventral (encircled by pink rectangle) and a dorsal module (encircled by yellow rectangle) in the navigation network. Right: Violin Fig.s for resting-state FC within each module and that between the two modules. Abbr. hippocampus (HIP), parahippocampus gyrus (PHG), retrosplenial complex (RSC), lingual gyrus (LING), fusiform gyrus (FFG), middle occipital gyrus (MOG), superior parietal gyrus (SPG), inferior parietal lobe (IPL), angular gyrus (ANG), precuneus (PCUN), precentral gyrus (PreCG), superior frontal gyrus (SFG), middle frontal gyrus (MFG), supplementary motor area (SMA).

as the critical values for the statistical significance with Type-I errors of 0.05.

In addition, for each node, we calculated its within- and between-module FC values for each participant. Then, we performed permutation tests to examine the group differences and Bonferroni correction was used for multiple comparisons.

2.4.4. Task-state fMRI data preprocessing and FC analysis

Image preprocessing of task-state fMRI data was performed with FEAT Version 6.00 (fMRI Expert Analysis Tool, part of FSL). For each participant, the first-level analysis was conducted separately on each run. Image preprocessing included motion correction, brain extraction, spatial smoothing (with a Gaussian kernel of 6 mm FWHM), intensity normalization, and high pass temporal filtering (120s cutoff). To remove physiological and other artifactual effects, the cerebrospinal fluid, white matter, six head motion correction parameters and first derivatives of these signals were used as potential confound regressors. In addition, we also regressed out the main condition effects (condition blocks convolved with *hrf*) to further avoid systematic influence by the proper-

ties of the generic task (Al-Aidroos et al., 2012; Westphal et al., 2017). After removing the effect of the defined confounds, we extracted the averaged residual time series with Fisher z-transformed from each region for each task condition (i.e., scene, face, object, scramble object, and fixation) in every block. Then we concatenated these segments across all runs, and correlated these time series across all pairs of identified regions for each condition and each participant. The resulting FC matrices of Pearson's *r* values for each participant were used for further analysis.

2.4.5. Age-related changes of the task modulation effects on the navigation network

We focused on scene-viewing task and investigated scene-related task-evoked development changes of navigation network. First, we calculated the within-ventral FCs, within-dorsal FCs and between-module FCs in the scene condition. Cole et al. (2014) have proposed that the task-based FC is shaped primarily by intrinsic network architecture with task-evoked network changes. Then, we estimated the task modulation effects by subtracting the resting-state FCs from the corresponding task-state FCs. As a result, we obtained the task modulation effects on within-

ventral, within-dorsal, and between-module FCs for each participant. Finally, we examined how the task modulation effects changed from children to adults by using permutation tests.

2.4.6. Control analyses

A series of control analyses were conducted to exclude possible confounding effects of head motion. First, we examined group differences in the head motion parameters (i.e., FD and DVARS) and performed the group comparison between children and adults by including FD and DVARS as covariates. Second, we matched children and adults on both mean FD and DVARS and re-performed the group comparisons in the matched sub-sample. Third, to minimize motion-related artefact in FC estimates, we further conducted the volume censoring (or “scrubbing”; Power et al., 2012) in preprocessing to exclude the volumes with excessive FD and DVARS for each child and adult participant under resting- and task-state respectively. The volumes with $FD > 0.3$ mm or $DVARS > 3\%$ were removed from analyses. A few volumes were eliminated at such threshold (for adults: 2.87 ± 5.77 volumes in resting state, 21.32 ± 17.75 volumes in task state; for children: 13.42 ± 19.22 volumes in resting state, 40.20 ± 28.26 volumes in task state). All participants had more than 5 minutes of valid BOLD data after scrubbing for both resting- and task-state scanning. The post-scrubbing data were used for further FC analyses.

In addition, we also performed control analyses to exclude the possible confounding factors, such as temporal signal to noise ratio (tSNR), template registered bias, and attention. First, we examined the group differences in temporal signal to noise (tSNR) calculated as the ratio between the temporal mean and standard deviation of the functional time series after pre-processing (Bennett and Miller, 2010; Krüger and Glover, 2001). Second, to rule out the template registration bias, we adopted the age-specific brain templates of Chinese children and adolescents (Dong et al., 2020) and registered the individual functional images of child participants to their corresponding age-specific templates. Then we repeated the following analyses to validate the results. Finally, to exclude the confounding effects of attention on the group differences in task modulation effects, we examined the activation differences in V1 when perceiving scenes between children and adults.

3. Results

3.1. Identifying the intrinsic modular structure of the navigation network

We used a meta-analysis approach, using Neurosynth, to define the regions involved in spatial navigation (Yarkoni et al., 2011; Hao et al., 2017; Kong et al., 2016a), and 23 regions distributed in the medial temporal, parietal, and frontal lobes were identified to constitute the navigation network (Table 1). Then, we explored the modular structure of the navigation network in adults by conducting a modularity analysis on the group-averaged resting-state FC matrix. An auto-generated optimal community structure of two modules was obtained, with a modularity index (Q value) of 0.45, indicating a strong modular division for the navigation network (Newman, 2004; Newman and Girvan, 2004). Thus, the navigation network was separated into two modules, with the ventral module containing 10 regions and the dorsal module containing 13 regions (see Methods and Table 1).

To further characterize the intrinsic modular structure of the navigation network in adults, we calculated the resting-state FC within each module (i.e., the averaged FC between each pair of regions) and that between the two modules (i.e., the averaged FC between each region in ventral module and each region in dorsal module). Both the ventral (mean = 0.65; $SD = 0.16$; one-sample t-test, $t_{259} = 65.02$; $p < 0.001$; Cohen's $d = 4.02$) and dorsal modules (mean = 0.35; $SD = 0.11$; one-sample t-test, $t_{259} = 63.62$; $p < 0.001$; Cohen's $d = 3.32$) exhibited strong positive within-module FCs, but the FCs between the two modules were negative (mean = -0.03; $SD = 0.11$; one-sample t-test, $t_{259} = -4.20$; $p < 0.001$; Cohen's $d = -0.26$) (Fig. 1A). Moreover, the resting-state FCs within both

modules were significantly stronger than that between modules (within-ventral vs. between: $t_{259} = 57.94$; $p < 0.001$; Cohen's $d = 4.92$; within-dorsal vs. between: $t_{259} = 39.28$; $p < 0.001$; Cohen's $d = 3.51$), indicating relative independence and segregation between the ventral and dorsal modules. Besides, the resting-state FC within the ventral module was stronger than that within the dorsal module ($t_{259} = 27.00$; $p < 0.001$; Cohen's $d = 2.21$), suggesting tighter integration within the ventral module than the dorsal module.

Notably, previous studies have found that the ventral and dorsal modules exhibited different cognitive functions and certain regions showed distinct development changes (Ofen et al., 2007; Scherf et al., 2007), which may be underpinned by diverse development changes of FC profiles in different modules (Mahon and Caramazza, 2011; Song et al., 2015). Thus, we next investigated the development of the intrinsic modular structure of the navigation network by examining the age-related changes of the resting-state FC profiles within and between the two modules.

3.2. Age-related changes of the intrinsic modular structure of the navigation network

First, we examined whether the navigation network in children showed similar modular structure as in adults. We performed the modularity analysis in children and found the same modular structure as in the adults. That is, an optimal structure of two modules was obtained, with a Q value of 0.39. As in adults, one module included 10 regions in the ventral temporal stream while the other module included 13 regions mainly in the frontal-dorsal stream. In addition, strong within-module FC (within-ventral: mean = 0.56, $SD = 0.13$, $t_{109} = 43.41$, $p < 0.001$, Cohen's $d = 3.48$; within-dorsal: mean = 0.36, $SD = 0.12$, $t_{109} = 31.83$, $p < 0.001$, Cohen's $d = 2.99$; Fig. 1B) and weak between-module FC (mean = 0.03, $SD = 0.11$, $t_{109} = 2.39$, $p < 0.018$, Cohen's $d = 0.27$; Fig. 1B) were observed. Paired sample t-tests showed that the resting-state FCs within both modules were stronger than that between modules (within-ventral vs. between: $t_{109} = 30.3$; $p < 0.001$; Cohen's $d = 4.28$; within-dorsal vs. between: $t_{109} = 21.99$; $p < 0.001$; Cohen's $d = 2.90$), and the resting-state FC within the ventral module was stronger than that within the dorsal module ($t_{109} = 11.59$; $p < 0.001$; Cohen's $d = 1.54$). These results suggested that the ventral and dorsal modules already showed functional segregation in children. The next question is whether children exhibited differences in the intrinsic modular structure of the navigation network compared with adults.

As shown in Fig. 2A, we found that adults showed stronger resting-state FC within the ventral module than children (permutation-test $P < 0.001$), suggesting tighter integration within the ventral module in adults than children. In addition, we found that most of the ventral module regions showed stronger averaged FCs with other ventral module regions in adults than in children (permutation-tests with Bonferroni correction: HIP.L: $P < 0.001$; HIP.R: $P < 0.001$; PHG.L: $P < 0.001$; PHG.R: $P < 0.001$; RSC.L: $P < 0.001$; RSC.R: $P < 0.001$; LING.L: $P = 0.005$; LING.R: $P < 0.001$; FFG.R: $P < 0.001$; FFG.L: $P = 0.04$), indicating that the age-related increases of within-ventral FC were universal among most ventral module regions. In contrast, no group difference was found for the resting-state FC within the dorsal module (adults: 0.35 ± 0.11 ; children: 0.36 ± 0.12 ; permutation-test $P = 0.39$), suggesting that children had adult-like integration within the dorsal module. That is, the ventral and dorsal modules showed dissociable age-group effects.

Interestingly, the resting-state FC between the ventral and dorsal modules was weaker in adults than in children (permutation-test $P < 0.001$, Fig. 2B). It was worth noting that the average between-module FC was positive in children but negative in adults. These results indicated that the ventral and dorsal modules tended to be more segregated with development.

Taken together, the navigation network might undergo a strengthening of the intrinsic modularity structure with age, with tighter integra-

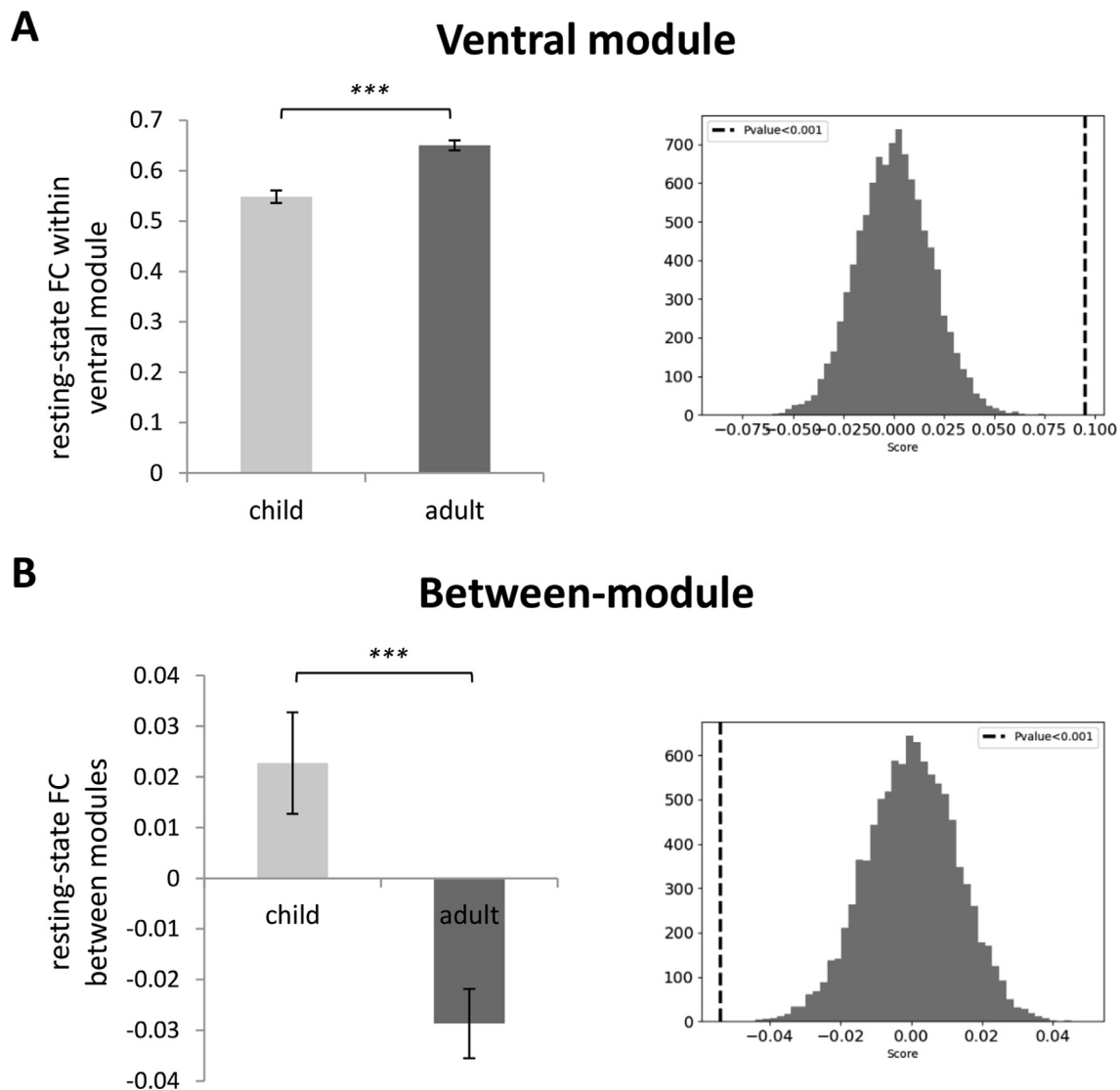


Fig. 2. Age-related changes in the resting-state FCs of the navigation network. A. Left: resting-state FC within the ventral module in adults and children; right: the permutation test. B. Left: resting-state FC between the ventral and dorsal modules in adults and children; right: the permutation test.

tion within the ventral module and more separation between the ventral and dorsal modules.

3.3. Task modulation of the modular structure of the navigation network

We further explored the task modulation of the modular structure of the navigation network during a scene viewing task. First, we found that the modularity of the navigation network under task-state was low in both adults and children (adults: $Q = 0.24$, children: $Q = 0.25$). Then, we calculated FC matrix during the scene viewing task and subtracted the resting-state FC matrix from the corresponding task-state FC matrix (Cole et al., 2014). As shown in Fig. 3A, for adults, compared with resting-state, the scene task significantly weakened the FC within the ventral module (mean = -0.16 , $SD = 0.18$; one-sample t -test, $p < 0.001$, Cohen's $d = -0.88$), but strengthened the FC between the ventral and dorsal modules (mean = 0.20 , $SD = 0.14$; $p < 0.001$, Cohen's $d = 1.40$) and that within the dorsal module (mean = 0.07 , $SD = 0.14$; $p < 0.001$, Cohen's $d = 0.53$). Similar task modulation effects were found in children (Fig. 3B), that is, the FCs were weakened within the ventral module (mean = -0.05 , $SD = 0.17$; $p < 0.001$, Cohen's $d = -0.30$), and strengthened between the ventral and dorsal modules (mean = 0.14 , $SD = 0.15$; $p < 0.001$, Cohen's $d = 0.90$) and within the dorsal module (mean = 0.08 ,

$SD = 0.15$; $p < 0.001$, Cohen's $d = 0.51$). Thus, the ventral module tended to be weakened while the dorsal module and integration between the two modules tended to be strengthened under task demands for both adults and children.

3.4. Age-related changes in task modulation of the navigation network

Next, we examined whether there were age-related differences in task modulation effects between adults and children. We found that the decrease of FC within the ventral module during task-state was greater in adults than in children (permutation-test $P < 0.001$, Fig. 4A). These results indicated that the scene viewing task weakened the integration within the ventral module from resting-state more in adults than in children. Task modulation in the within-dorsal module did not show a significant difference between adults and children (permutation-test $P = 0.82$). In addition, we observed that the increase of FC between the ventral and dorsal modules was greater in adults than in children (permutation-test $P < 0.001$, Fig. 4B), suggesting that adults strengthened the interactions between the two modules during task-state more than children. In short, the age-related changes in task modulation effect from children to adults indicated that adults were more flexible than children to break up the intrinsic modular structure under task-state.

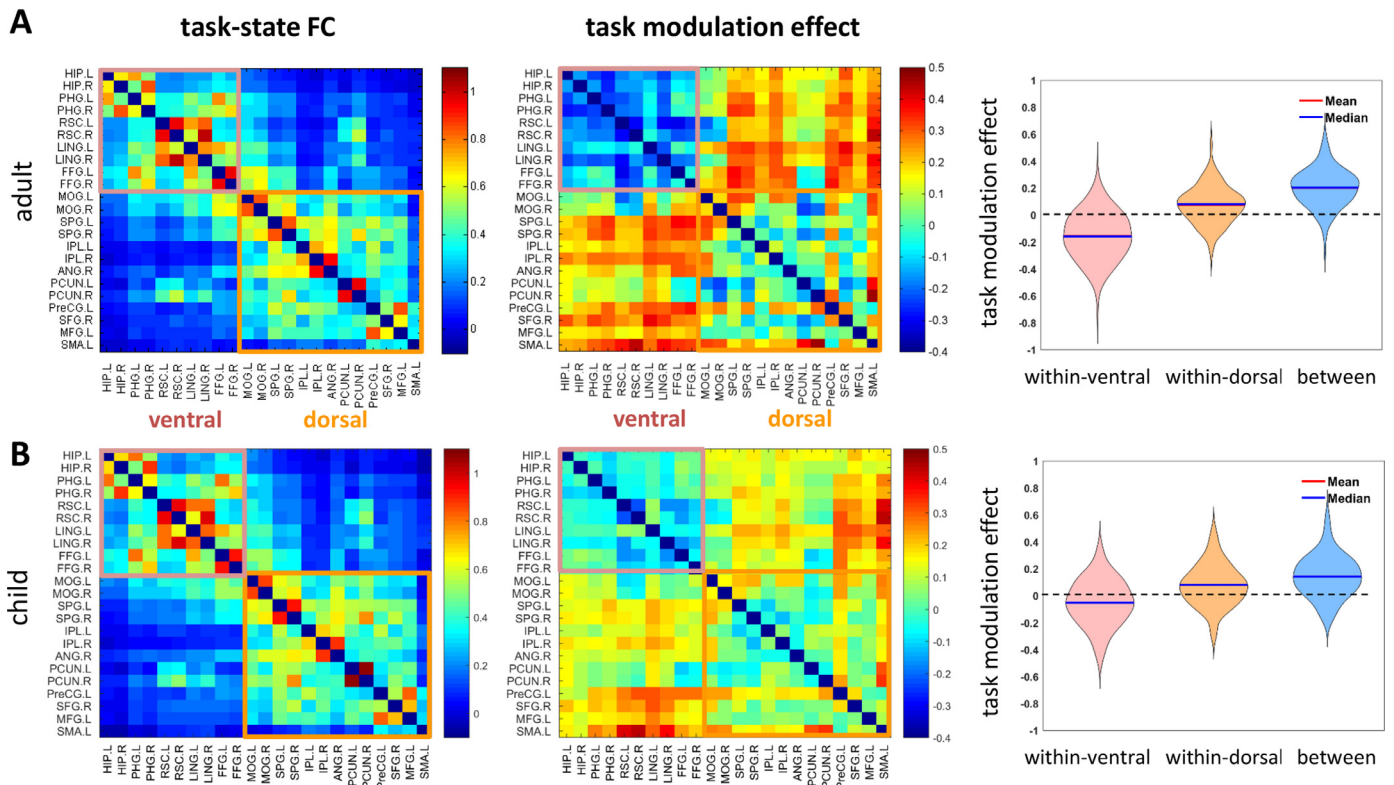


Fig. 3. Task-state FC profiles and task modulation of FCs in the navigation network in adults (A) and children (B). The group-averaged task-state FC matrix (left) and task modulation of FC matrix (middle) of navigation network. Right: violin Figs for task modulation of FC within each module and that between the two modules.

Table 2
mean FD and DVARS under resting-state and task-state for adults and children (mean ± SD).

	Resting state		Task state	
	FDs	DVARS (%)	FDs	DVARS (%)
Adults	0.10 ± 0.03	1.12 ± 0.31	0.09 ± 0.03	1.19 ± 0.32
Children	0.13 ± 0.05	1.36 ± 0.39	0.12 ± 0.05	1.48 ± 0.44

Next, we asked whether the task modulation effects on the modular structure depended on the specific task of perceiving scenes. We examined the task-related FC changes in the object- and face-viewing conditions. The results showed that for children, the modular structure was modulated when viewing scenes, but not when viewing objects or faces. In contrast, for adults, similar task-related changes in modular structure were observed in all three conditions. In short, the task-related changes in modular structure depended on the specific task in children, but not in adults (Supplementary analysis 1).

3.4.1. Control analyses on head motion

Given that the difference in head motion between children and adults is a potentially major confounding factor in our study, we performed a series of comprehensive control analysis to address the motion issue.

In our study, children tended to show higher mean FD and DVARS than adults under both resting- and task-state (permutation-test $P_s < 0.001$, Table 2). Therefore, we re-performed the permutation test to examine the group differences in FCs by including the FD and DVARS as covariates, and the results remained unchanged (Supplementary analysis 2).

Then, we matched children and adults on both FD and DVARS by excluding children with high head motion and adults with low head motion (i.e., remaining 67 children and 199 adults). As a result, there was no significant group difference in mean FD or DVARS under resting-

or task-state (permutation test $P_s > 0.05$, Supplementary Table). All the results were replicated in the matched sub-sample (Supplementary analysis 2).

Further, we conducted volume censoring in preprocessing to exclude the volumes with excessive FD and DVARS for each child and adult participant under resting- and task-state respectively. All the results were replicated in the censored data. Under resting-state, the same optimal structure of two modules was obtained in adults ($Q = 0.446$) and children ($Q = 0.405$), with strong within-module FC (within-ventral, adults: 0.65 ± 0.16 , $p < 0.001$, Cohen's $d = 4.05$, children: 0.54 ± 0.13 , $p < 0.001$, Cohen's $d = 4.13$; within-dorsal, adults: 0.35 ± 0.11 , $p < 0.001$, Cohen's $d = 2.18$, children: 0.37 ± 0.12 , $p < 0.001$, Cohen's $d = 3.07$, Supplementary Fig. 3) and weak between-module FC observed (adults: -0.03 ± 0.11 , $p < 0.001$, Cohen's $d = -0.27$, children: 0.02 ± 0.11 , $p < 0.05$, Cohen's $d = 0.18$, Supplementary Fig. 3). Importantly, adults showed higher within-ventral FC (permutation-test $P < 0.001$, regressing out FD and DVARS, Supplementary Fig. 4) and lower between-module FC than children (permutation-test $P = 0.002$, regressing out FD and DVARS, Supplementary Fig. 4). No group difference was found for the within-dorsal FC (permutation-test $P = 0.91$, regressing out FD and DVARS). Under task-state, compared with resting-state, the within-ventral FC was weakened (adults: -0.16 ± 0.18 , $p < 0.001$, Cohen's $d = -0.90$; children: -0.03 ± 0.18 , $p = 0.08$, Cohen's $d = -0.16$, Supplementary Fig. 5), but the between-module FC was strengthened (adults: 0.20 ± 0.14 , $p < 0.001$, Cohen's $d = 1.42$; children: 0.15 ± 0.15 , $p < 0.001$, Cohen's $d = 0.99$, Supplementary Fig. 5), and the within-dorsal FC was also strengthened (adults: 0.08 ± 0.14 , $p < 0.001$, Cohen's $d = 0.58$; children: 0.07 ± 0.15 , $p < 0.001$, Cohen's $d = 0.49$, Supplementary Fig. 5). Importantly, both decrease of within-ventral FC and increase of between-module FC was greater in adults than in children (within-ventral, permutation-test $P < 0.001$, between-module: $P = 0.001$, regressing out FD and DVARS, Supplementary Fig. 6). No group difference of task modulation effect was found for the within-dorsal FC (permutation-test $P = 0.37$, regressing out FD and DVARS).

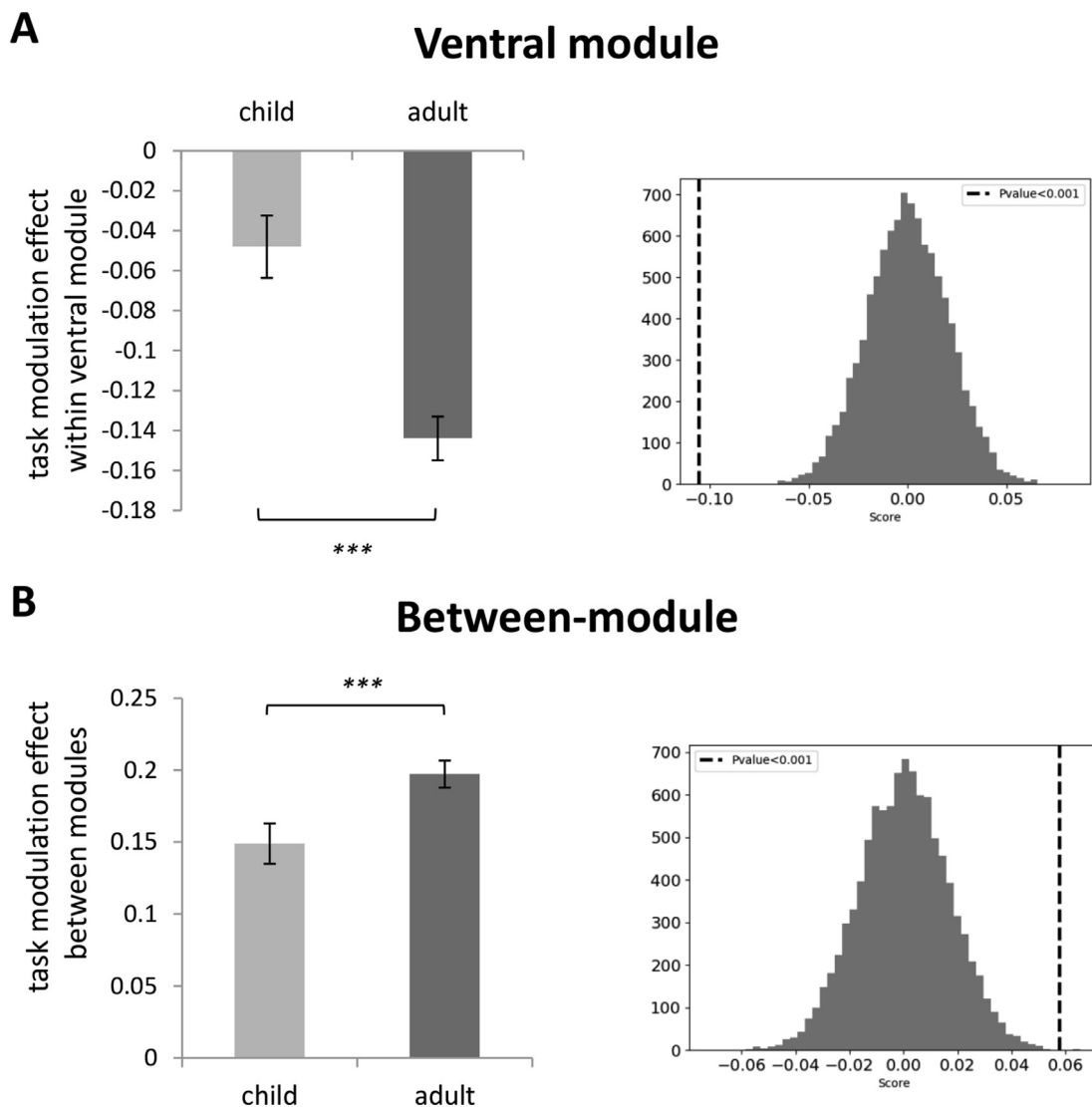


Fig. 4. Age-related changes in the task modulation of FCs in the navigation network. A. Left: task modulation of FC within the ventral module in adults and children; right: the permutation test. B. Left: task modulation of FC between the ventral and dorsal modules during task-state in adults and children; right: the permutation test.

3.4.2. Other control analyses

We also performed control analyses to ensure that the age-related FC changes were not caused by confounding factors such as tSNR, template registration bias, and attention. First, we calculated the tSNR in the identified navigation network for each participant (Supplementary Table 2), and found that the tSNR values did not differ between children and adults under resting-state (permutation-test $P = 0.34$) or task-state (permutation-test $P = 0.11$). Further, we compared the tSNR between children and adults in the ventral and dorsal modules (Supplementary Table 2). There was no significant difference between the two groups in the ventral module (resting-state: permutation-test $P = 0.42$; task-state: permutation-test $P = 0.80$). In the dorsal module, the tSNR did not differ under resting-state (permutation-test $P = 0.31$), but showed a difference under task-state (permutation-test $P < 0.001$). Therefore, we re-performed the analysis to test the group differences regarding the dorsal module after regressing out the tSNR, and the results remained unchanged. That is, the increase of between-module FC under task-state was greater in adults than in children (permutation-test $P < 0.001$), and the task modulation effect within the dorsal module did not differ between adults and children (permutation-test $P = 0.57$). Thus, our results could not be accounted for by tSNR difference between children and adults.

Second, further control analyses showed that the main findings could not be explained by the template registration bias. We registered functional data of the children to their age-specific templates (Dong et al., 2020) and similar pattern of age-related changes in network organization as the main findings was obtained. (Supplementary analysis 3).

Third, control analysis showed that there was no group difference in activation in V1 when perceiving scenes (Supplementary analysis 4), suggesting that the group differences in task modulation effects were not caused by attention differences between groups.

4. Discussion

The present study investigated the development of functional organization of the whole navigation network during both resting- and task-states. We first identified the intrinsic modular structure in the navigation network that included a ventral and a dorsal module. Then, we found that the intrinsic modular structure was strengthened during development, that is, adults showed stronger resting-state FC within the ventral module and weaker resting-state FC between ventral and dorsal modules than children. Further, the intrinsic modular structure was loosened when performing scene-viewing task, that is, both adults and children showed decreased FC within the ventral module and increased

FC between the ventral and dorsal modules during task-state compared with resting-state. Finally, the FC changes modulated by task demands were greater in adults than in children, suggesting that the navigation network in adults could more flexibly loosen the intrinsic modular structure in response to task demands. In sum, our study reveals the age-related changes in navigation network organization as a process of increasing modularity under resting-state and increasing flexibility under task-state.

In our study, we found similar intrinsic modular structure of the navigation network in adults and children. In addition, comparable task modulation effects on the modular structure were observed for adults and children. Such similarities in intrinsic organization and task modulation effects between adults and children suggest that the navigation network of the 10-13-year-old children has developed to some extent. These results are consistent with general neurodevelopmental findings that brain networks are reorganized by degree, rather than by radical topological changes, during late-childhood and adolescence (Stevens, 2016).

Despite that, there were substantial age-related differences in both intrinsic organization and task modulation of navigation network between adults and children. First, we found that adults showed higher FC within the ventral module and lower FC between the two modules, indicating that the intrinsic modular structure was strengthened from children to adults. So far, previous resting-state FC studies have achieved fruitful findings on developmental reorganization of different functional networks. For example, the control system comprises two separate networks in adults but shows intertwined architecture in adolescents and children (Fair et al., 2007). The default mode network is a cohesive, interconnected network in adults but sparsely connected in children (Fair et al., 2008). The reconfiguration of the face network with age shows simultaneous increased FC within the core face network and decreased FC between the core and extended face networks (Wang et al., 2017). Consistent with other functional networks, we found that the developmental reorganization of the navigation network was accompanied by both within-module integration and between-module segregation. This development of network structure may drive the functional specialization of the ventral module regions in navigation network, according to the interactive specialized view (Johnson, 2011). Specifically, the ventral module identified in our study contained the HIP and the scene-selective regions, such as the PPA, RSC, which are widely recognized as critical regions for navigation. From children to adults, these ventral module regions may become more efficient to integrate navigation-related information among them to sharpen its functionality and, meanwhile, segregate information flow between the ventral and dorsal modules to eliminate irrelevant information. Interestingly, the dissociable development of ventral and dorsal subnetworks was also found in the attention network (Farrant and Uddin, 2015).

Further, we found that the scene-viewing task reduced within-module FC and enhanced between-module FC for both adults and children. These results indicated weakening of the intrinsic modular structure in response to the task demands, which promotes communication between ventral and dorsal modules. This flexible adaptation to meet task demands is in line with previous studies on task-state network connectivity (Bullmore and Sporns, 2012; Cassidy et al., 2016; Vatansever et al., 2015). For example, the global brain modularity decreases and inter-network interactions increases in response to greater cognitive load in working memory task (Vatansever et al., 2015).

More importantly, we found that adults are more flexible in response to task demands than children, as evidenced by the greater task modulation effects on network structure in adults than in children. That is, adults showed greater decrease of within-module FC and greater enhancement of between-module FC from resting-state to task-state than children. The existing research on navigational network development has mainly examined age-related changes in interactions between individual regions, rather than global network organization. For example, during a scene recognition task, the connectivity between the left en-

torhinal sub-regions and the left dorsolateral prefrontal cortex increased with age (Menon et al., 2005). In addition, the FC between the left PHG and left inferior frontal gyrus positively correlated with age in scene retrieval task (Ofen et al., 2012). These results illuminate that the interactions between the MTL in ventral module and prefrontal cortex in dorsal module increases with age under navigational tasks, consistent with our result that between-module interactions increase more in adults than in children. Beyond that, we found that the FC within the ventral module decreased more in adults than in children. These two aspects of development trends of task modulation effects are complementary to each other. Adults may be more flexible to break the modular balance under resting-state in response to task demands, which promoted the informative efficiency between the two modules during task-state.

Taken together, our results revealed that on the one hand, children aged 10-13 years already showed similar two-modular structure of the navigation network as adults, while on the other hand, there were still differences in intrinsic network organization and task modulation between children and adults. Interestingly, a body of behavioral studies have shown adult-like performances in some navigation tasks around 11-12 years of age (Bullens et al., 2010; Burles et al., 2020; Nardini et al., 2008; Nazareth et al., 2018). These findings suggest the possibility of a coarse acquisition of navigation skills in childhood and a prolonged fine-tuning of these skills until adulthood (Nazareth et al., 2018; Burles et al., 2020), which may be related to the delayed maturation of underlying neural basis. It is possible that the changes of the navigation network organization are both providing the drives for and afforded by the changes in navigational behaviors.

In sum, our study reveals the developmental changes of the navigation network organization as a process of increasing modularity under resting-state and increasing flexibility under task-state. Several issues are unaddressed in the present study that should be addressed in future research. First, we did not observe any differences in FC within the dorsal module between the 10-13 year-old children and adults, and further studies are needed to explore whether the dorsal module develops at an earlier age. Second, considering the complexity of spatial navigation, we tentatively focused on scene perception, the critical component of navigation, to explore the age-related changes in task modulation effect. Although the brain regions involved in scene processing and navigation may overlap to a great extent, it does not guarantee that the whole navigation network was activated under the scene viewing task in our study. Thus, cautious should be taken when generalizing the current findings of task modulation effect to other navigational tasks. Future studies are needed to use more delicate and multifaceted navigational tasks to examine the difference in task modulation effects between children and adults. Third, Data in task- and resting-state differed in scan length and acquisition parameters, and more volumes were excluded after censoring in task-state than resting-state, which may be due to longer scan time or task demands. Therefore, the difference in FCs between task- and resting-state might be partly confounded with the differences in fMRI data between the two states. Forth, previous studies have demonstrated that the anatomical connection precedes and instructs FC development (Meissner et al., 2021; Saygin et al., 2012; Saygin et al., 2016), and further longitudinal research is needed to investigate how the development of anatomical connection in the navigation network guides the development of intrinsic and task-evoked FC and related navigation behavior. Finally, many studies have demonstrated that gifted children possess superior spatial ability than normal children (Myers et al., 2017), which provides a window to investigate how the developmental reorganization of the navigation network may underlie the growth of spatial ability.

Declaration of Competing Interest

The authors declare no competing financial interests.

Credit Author Statement

Xin Hao, Yiying Song, and Jia Liu designed the experiments, Xin Hao and Xiangzhen Kong conducted the experiments, Xin Hao and Taicheng Huang analyzed the data, Xin Hao and Yiying Song wrote the manuscript, Yiying Song, and Jia Liu supervised the project.

Data and Code Availability Statement

The data in our study comes from an ongoing project (Gene Environment Brain & Behavior).

Both data and code are available upon request. The Data-Sharing and Usage Agreement will be signed between the user and provider (Gene Environment Brain & Behavior Project, directed by Dr. Jia Liu) of data. In particular, the user should agree to the following terms, including using the database only for academic research, protecting the participants' information, not release data to a third party without approval, and so on.

The data sharing is in compliance with the standards of the Institutional Review Board of Beijing Normal University and funding agreement.

The data are still accumulating and the means of data sharing in public repositories have not been fully discussed yet. Thus, I am not uploading our data, but we agree that eventually the data shall be put in public repositories.

Acknowledgments

This study was funded by the National Natural Science Foundation of China (31872786, 31861143039), the National Basic Research Program of China (2018YFC0810602), the Natural Science Foundation of Hubei Province of China (2020CFB363), and the Open Research Fund of the Key Laboratory of Adolescent Cyberpsychology and Behavior (CCNU) (2019A01).

Supplementary materials

Supplementary material associated with this article can be found, in the online version, at doi:10.1016/j.neuroimage.2021.118515.

References

- Al-Aidroos, N., Said, C.P., Turk-Browne, N.B., 2012. Top-down attention switches coupling between low-level and high-level areas of human visual cortex. *Proc. Natl Acad. Sci. USA* 109, 14675–14680.
- Baldassano, C., Beck, D.M., Fei-Fei, L., 2013. Differential connectivity within the parahippocampal place area. *Neuroimage* 75, 228–237.
- Baldassano, C., Esteva, A., Fei-Fei, L., Beck, D.M., 2016. Two distinct scene-processing networks connecting vision and memory. *eNeuro* 3, 0178–0116.
- Bennett, C.M., Miller, M.B., 2010. How reliable are the results from functional magnetic resonance imaging? *Ann. N. Y. Acad. Sci.* 1191, 133–155.
- Biswal, B., Zerrin, Y.F., Haughton, V.M., Hyde, J.S., 1995. Functional connectivity in the motor cortex of resting human brain using echo-planar MRI. *Magn. Reson. Med.* 34, 537–541.
- Biswal, B.B., Mennes, M., Zuo, X.N., Gohel, S., Kelly, C., Smith, S.M., Beckmann, C.F., Adelman, J.S., Buckner, R.L., Colcombe, S., et al., 2010. Toward discovery science of human brain function. *Proc. Natl Acad. Sci. USA* 107, 4734–4739.
- Boccia, M., Sulpizio, Nemmi F., Guariglia, C., Galati, G., 2016. Direct and indirect parieto-medial temporal pathways for spatial navigation in humans: evidence from resting-state functional connectivity. *Brain Struct. Funct.* 222, 1945–1957.
- Bonner, M.F., Epstein, R.A., 2017. Coding of navigational affordances in the human visual system. *Proc. Natl Acad. Sci. USA* 114, 4793–4798.
- Brown, T.L., Carr, V.A., LaRocque, K.F., Favila, S.E., Gordon, A.M., Bowles, B., Bailenson, J.N., Wagner, A.D., 2016. Prospective representation of navigational goals in the human hippocampus. *Science* 352, 1323–1326.
- Bullens, J., Igló, K., Berthoz, A., Postma, A., Rondi-Reig, L., 2010. Developmental time course of the acquisition of sequential egocentric and allocentric navigation strategies. *J. Exp. Child. Psychol.* 107, 337–350.
- Bullmore, E., Sporns, O., 2012. The economy of brain network organization. *Nat. Rev. Neurosci.* 13, 336–349.
- Burgess, N., 2006. Spatial memory: how egocentric and allocentric combine. *Trends Cogn. Sci.* 10, 551–557.
- Burles, F., Liu, I., Hart, C., Murias, K., Graham, S.A., Iaria, G., 2020. Mergence of Cognitive Maps for Spatial Navigation in 7- to 10-Year-Old Children. *Child Dev.* 91, e733–e744.

- Cassidy, C.M., Van Snellenberg, J.X., Benavides, C., Slifstein, M., Wang, Z., Moore, H., Abi-Dargham, A., Horga, G., 2016. Dynamic connectivity between brain networks supports working memory: relationships to dopamine release and schizophrenia. *J. Neurosci.* 36, 4377–4388.
- Chai, X.J., Ofen, N., Jacobs, L.F., Gabrieli, J.D., 2010. Scene complexity: influence on perception, memory, and development in the medial temporal lobe. *Front. Hum. Neurosci.* 4, 21.
- Ciric, R., Wolf, D.H., Power, J.D., Roalf, D.R., Baum, G.L., Ruparel, K., et al., 2017. Benchmarking of participant-level confound regression strategies for the control of motion artifact in studies of functional connectivity. *Neuroimage* 1, 174–187.
- Cole, M.W., Bassett, D.S., Power, J.D., Braver, T.S., Petersen, S.E., 2014. Intrinsic and task-evoked network architectures of the human brain. *Neuron* 83, 238–251.
- Dong, H.M., Castellanos, F.X., Yang, N., Zhang, Z., Zhou, Q., He, Y., et al., 2020. Charting brain growth in tandem with brain templates at school age. *Sci. Bull.* 65, 1924–1934.
- Epstein, R.A., Patai, E.Z., Julian, J.B., Spiers, H.J., 2017. The cognitive map in humans: spatial navigation and beyond. *Nat. Neurosci.* 20, 1504–1513.
- Epstein, R.A., Vass, L.K., 2014. Neural systems for landmark-based wayfinding in humans. *Phil. Trans. R. Soc. B* 369, 20120533.
- Fair, D.A., Cohen, A.L., Dosenbach, N.U., Church, J.A., Miezin, F.M., Barch, D.M., Raichle, M.E., Petersen, S.E., Schlaggar, B.L., 2008. The maturing architecture of the brain's default network. *Proc. Natl Acad. Sci. USA* 105, 4028–4032.
- Fair, D.A., Dosenbach, N.U., Church, J.A., Cohen, A.L., Brahmbhatt, S., Miezin, F.M., Barch, D.M., Raichle, M.E., Petersen, S.E., Schlaggar, B.L., 2007. Development of distinct control networks through segregation and integration. *Proc. Natl Acad. Sci. USA* 104, 13507–13512.
- Farrant, K., Uddin, L.Q., 2015. Asymmetric development of dorsal and ventral attention networks in the human brain. *Dev. Cogn. Neurosci.* 12, 165–174.
- Fox, M.D., Raichle, M.E., 2007. Spontaneous fluctuations in brain activity observed with functional magnetic resonance imaging. *Nat. Rev. Neurosci.* 8, 700–711.
- Fox, M.D., Snyder, A.Z., Vincent, J.L., Corbetta, M., Van Essen, D.C., Raichle, M.E., 2005. The human brain is intrinsically organized into dynamic, anticorrelated functional networks. *Proc. Natl Acad. Sci. USA* 102, 9673–9678.
- Golarai, G., Ghahremani, D.G., Whitfield-Gabrieli, S., Reiss, A., Eberhardt, J.L., Gabrieli, J.D., Grill-Spector, K., 2007. Differential development of high-level visual cortex correlates with category-specific recognition memory. *Nat. Neurosci.* 10, 512–522.
- Hao, X., Huang, Y., Li, X., Song, Y., Kong, X., Wang, X., Yang, Z., Zhen, Z., Liu, J., 2016. Structural and functional neural correlates of spatial navigation: a combined voxel-based morphometry and functional connectivity study. *Brain Behav.* 6, e00572.
- Hao, X., Wang, X., Song, Y., Kong, X., Liu, J., 2017. Dual roles of the hippocampus and intraparietal sulcus in network integration and segregation support scene recognition. *Brain Struct. Funct.* 223, 1473–1485.
- Helmfstein, S.M., Schonberg, T., Congdon, E., Karlsgodt, K.H., Mumford, J.A., Sabb, F.W., Cannon, T.D., London, E.D., Bilder, R.M., Poldrack, R.A., 2014. Predicting risky choices from brain activity patterns. *Proc. Natl Acad. Sci. USA* 111, 2470–2475.
- Jiang, P., Tokariev, M., Aronen, E.T., Salonen, O., Ma, Y., Vuontela, V., Carlson, S., 2014. Responsiveness and functional connectivity of the scene-sensitive retrosplenial complex in 7–11-year-old children. *Brain Cogn.* 92, 61–72.
- Johnson, M.H., 2011. Interactive specialization: a domain-general framework for human functional brain development? *Dev. Cogn. Neurosci.* 1, 7–21.
- Julian, J.B., Kamps, F.S., Epstein, R.A., Dilks, D.D., 2019. Dissociable spatial memory systems revealed by typical and atypical human development. *Dev. Sci.* 22, e12737.
- Julian, J.B., Ryan, J., Hamilton, R.H., Epstein, R.A., 2016. The occipital place area is causally involved in representing environmental boundaries during navigation. *Curr. Biol.* 26, 1104–1109.
- Kamps, F.S., Lall, V., Dilks, D.D., 2016. The occipital place area represents first-person perspective motion information through scenes. *Cortex* 83, 17–26.
- Kong, X., Wang, X., Pu, Y., Huang, L., Hao, X., Zhen, Z., Liu, J., 2016a. Human navigation network: the intrinsic functional organization and behavioral relevance. *Brain Struct. Funct.* 222, 749–764.
- Kong, X., Song, Y., Zhen, Z., Liu, J., 2016b. Genetic variation in S100B modulates neural processing of visual scenes in Han Chinese. *Cereb. Cortex* 27, 1326–1336.
- Kravitz, D.J., Saleem, K.S., Baker, C.I., Mishkin, M., 2011. A new neural framework for visuospatial processing. *Nat. Rev. Neurosci.* 12, 217–230.
- Krüger, G., Glover, G.H., 2001. Physiological noise in oxygenation-sensitive magnetic resonance imaging. *Magn. Reson. Med.* 46, 631–637.
- Lebedev, A.V., Westman, E., Simmons, A., Lebedeva, A., Siepel, F.J., Pereira, J.B., Aarsland, D., 2014. Large-scale resting state network correlates of cognitive impairment in Parkinson's disease and related dopaminergic deficits. *Front. Syst. Neurosci.* 8.
- Mahon, B.Z., Caramazza, A., 2011. What drives the organization of object knowledge in the brain? *Trends Cogn. Sci.* 15, 97–103.
- Meissner, T.W., Nordt, M., Weigelt, S., 2019. Prolonged functional development of the parahippocampal place area and occipital place area. *Neuroimage* 191, 104–115.
- Meissner, T.W., Genç, E., Mädler, B., Weigelt, S., 2021. Myelin development in visual scene-network tracts beyond late childhood: A multimethod neuroimaging study. *Cortex* 137, 18–34.
- Menon, V., Boyett-Anderson, J.M., Reiss, A.L., 2005. Maturation of medial temporal lobe response and connectivity during memory encoding. *Cognit. Brain Res.* 25, 379–385.
- Myers, T., Carey, E., Szűcs, D., 2017. Cognitive and neural correlates of mathematical giftedness in adults and children: a review. *Front. Psychol.* 8, 1646.
- Nardini, M., Jones, P., Bedford, R., Braddick, O., 2008. Development of cue integration in human navigation. *Curr. Biol.* 18, 689–693.
- Nazareth, A., Weisberg, S.M., Margulis, K., Newcombe, N.S., 2018. Charting the development of cognitive mapping. *J. Exp. Child. Psychol.* 170, 86–106.
- Newman, M.E.J., 2004. Fast algorithm for detecting community structure in networks. *Phys. Review E* 69, 066133.

- Newman, M.E.J., Girvan, M., 2004. Finding and evaluating community structure in networks. *Phys. Rev. E* 69, 026113.
- Nichols, T.E., Holmes, A.P., 2002. Nonparametric permutation tests for functional neuroimaging: a primer with examples. *Hum. Brain Mapp.* 15, 1–25.
- Ofen, N., Chai, X.J., Schuil, K.D., Whitfield-Gabrieli, S., Gabrieli, J.D., 2012. The development of brain systems associated with successful memory retrieval of scenes. *J. Neurosci.* 32, 10012–10020.
- Ofen, N., Kao, Y.-C., Sokol-Hessner, P., Kim, H., Whitfield-Gabrieli, S., Gabrieli, J.D., 2007. Development of the declarative memory system in the human brain. *Nat. Neurosci.* 10, 1198–1205.
- Parkes, L., Fulcher, B., Yücel, M., Fornito, A., 2018. An evaluation of the efficacy, reliability, and sensitivity of motion correction strategies for resting-state functional MRI. *Neuroimage* 1, 415–436.
- Power, J.D., Barnes, K.A., Snyder, A.Z., Schlaggar, B.L., Petersen, S.E., 2012. Spurious but systematic correlations in functional connectivity MRI networks arise from subject motion. *Neuroimage* 59, 2142–2154.
- Rubinov, M., Sporns, O., 2010. Complex network measures of brain connectivity: uses and interpretations. *Neuroimage* 52, 1059–1069.
- Saygin, Z.M., Osher, D.E., Koldewyn, K., Reynolds, G., Gabrieli, J.D., Saxe, R.R., 2012. Anatomical connectivity patterns predict face selectivity in the fusiform gyrus. *Nat. Neurosci.* 15, 321–327.
- Saygin, Z.M., Osher, D.E., Norton, E.S., Youssoufian, D.A., Beach, S.D., Feather, J., Gaab, N., Gabrieli, J.D.E., Kanwisher, N., 2016. Connectivity precedes function in the development of the visual word form area. *Nat. Neurosci.* 19, 1250–1255.
- Scherf, K.S., Behrmann, M., Humphreys, K., Luna, B., 2007. Visual category-selectivity for faces, places and objects emerges along different developmental trajectories. *Dev. Sci.* 10, F15–F30.
- Song, Y., Zhu, Q., Li, J., Wang, X., Liu, J., 2015. Typical and atypical development of functional connectivity in the face network. *J. Neurosci.* 35, 14624–14635.
- Spiers, H.J., Barry, C., 2015. Neural systems supporting navigation. *Curr. Opin. Behav. Sci.* 1, 47–55.
- Stevens, M.C., 2016. The contributions of resting state and task-based functional connectivity studies to our understanding of adolescent brain network maturation. *Neurosci. Biobehav. R* 70, 13–32.
- Tzourio-Mazoyer, N., Landeau, B., Papathanassiou, D., Crivello, F., Etard, O., Delcroix, N., Mazoyer, B., Joliot, M., 2002. Automated anatomical labeling of activations in SPM using a macroscopic anatomical parcellation of the MNI MRI single-subject brain. *Neuroimage* 15, 273–289.
- Ungerleider, L., Mishkin, M., 1982. Two cortical visual systems. *Anal. Visual Behav.* 549–586.
- Vatansver, D., Menon, D.K., Manktelow, A.E., Sahakian, B.J., Stamatakis, E.A., 2015. Default mode dynamics for global functional integration. *J. Neurosci.* 35, 15254–15262.
- Wang, X., Zhen, Z., Song, Y., Huang, L., Kong, X., Liu, J., 2016. The hierarchical structure of the face network revealed by its functional connectivity pattern. *J. Neurosci.* 36, 890–900.
- Wang, X., Zhu, Q., Song, Y., Liu, J., 2017. Developmental reorganization of the core and extended face networks revealed by global functional connectivity. *Cereb. Cortex* 28, 3521–3530.
- Westphal, A.J., Wang, S., Rissman, J., 2017. Episodic memory retrieval benefits from a less modular brain network organization. *J. Neurosci.* 37, 3523–3591.
- Whitfield-Gabrieli, S., Nieto-Castanon, A., 2012. Conn: a functional connectivity toolbox for correlated and anticorrelated brain networks. *Brain Connect.* 2, 125–141.
- Yarkoni, T., Poldrack, R.A., Nichols, T.E., Van Essen, D.C., Wager, T.D., 2011. Large-scale automated synthesis of human functional neuroimaging data. *Nat. Methods* 8, 665–670.
- Zhen, Z., Yang, Z., Huang, L., Kong, X., Wang, X., Dang, X., Huang, Y., Song, Y., Liu, J., 2015. Quantifying interindividual variability and asymmetry of face-selective regions: a probabilistic functional atlas. *Neuroimage* 113, 13–25.
- Zhen, Z., Kong, X.Z., Huang, L., Yang, Z., Wang, X., Hao, X., Huang, T., Song, Y., Liu, J., 2017. Quantifying the variability of scene-selective regions: interindividual, inter-hemispheric, and sex differences. *Hum. Brain Mapp.* 38, 2260–2275.